



Structural Properties of Thermoluminescence Dosimeter Materials, Preparation, Application, and Adaptability: A Systematic Review

*^{1,2}EFENJI, GI; ¹ISKANDAR, SM.; ¹YUSOF, NN; ²RABBA, JA; ⁵MUSTAPHA, OI; ¹FADHIRUL, IM; ³UMAR, SA; ⁴KAMGBA, FA; ⁴USHIE, PO; ¹MUNIRAH, J; ¹THAIR, HK; ¹NABASU, SE; ¹HAYDER, SN; ^{1,6}OKE, AO

¹School of Physics, Universiti Sains Malaysia, 11800 USM, Penang, Malaysia.

²Department of Physics, Federal University Lokoja P.M.B. 1154 Kogi State Nigeria.

³Department of Physics, Federal University Lafia P.M.B. 146, Lafia Nigeria.

⁴Department of Physics, Cross River University of technology PMB 1123, Calabar.

⁵Department of Pure and Industrial Chemistry, Kogi State University (Prince Abubakar Audu University) Anyigba, Nigeria.

⁶Department of Physics, Federal University Oye-Ekiti, 373, Ekiti State, Nigeria.

*Corresponding Author Email: godwin.efenji@fulokoja.edu.ng

*ORCID: <https://orcid.org/0000/0002/14262111>

*Tel: +2347067022609

Co-Authors Email: iskandarshah@usm.my; nurnabihah7@usm.my; james.rabba@fulokoja.edu.ng; idrismustapha710@gmail.com; fadhirul@usm.my; usaltilde@yahoo.com; fkamgba@gmail.com; pat205ushie@unicross.edu.ng; munirah_jamil@yahoo.com; khaaalah@yahoo.com; 1982isseth@gmail.com; hayder985@student.usm.my; aduragbemi.oke@fuoye.edu.ng

ABSTRACT: Thermoluminescence dosimeters (TLDs) are widely used in radiation dosimetry due to their excellent properties, such as high sensitivity, small size, and ability to measure low doses of radiation. This review focuses on the structural properties of TLD materials, as well as their preparation, application, and adaptability. The review covers the various types of TLD materials, crystal structure, and properties, including energy response and fading characteristics. The different methods used to prepare TLD materials, such as solid-state synthesis, sol-gel synthesis, and solution growth methods, are discussed in detail. The review also includes a detailed discussion of the various applications of TLDs, including medical, environmental, and industrial radiation dosimetry. Extensive information on TLD is reviewed, and the TL characteristics that have a noticeable impact on the TL dosimetry potential for human and other purpose utilisation, such as mineral, oil, and gas resource investigation, can be done using natural and artificial TL signals. Information on TL measurement process requirements and the TL characteristics that have a noticeable impact on a compound TL dosimetry potential are also addressed. Finally, the review concludes by highlighting the adaptability of TLD materials to different dosimetry applications and their potential use in the future.

DOI: <https://dx.doi.org/10.4314/jasem.v28i4.13>

Open Access Policy: All articles published by **JASEM** are open-access articles and are free for anyone to download, copy, redistribute, repost, translate and read.

Copyright Policy: © 2024. Authors retain the copyright and grant **JASEM** the right of first publication with the work simultaneously licensed under the **Creative Commons Attribution 4.0 International (CC-BY-4.0) License**. Any part of the article may be reused without permission provided that the original article is cited.

Cite this Article as: EFENJI, G. I; ISKANDAR, S. M; YUSOF, N. N; RABBA, J. A; MUSTAPHA, O. I; FADHIRUL, I. M; UMAR, S. A; KAMGBA, F. A; USHIE, P. O; MUNIRAH, J; THAIR, H. K; NABASU, S. E; HAYDER, S. N OKE, A O. (2024). Structural Properties of Thermoluminescence Dosimeter Materials, Preparation, Application, and Adaptability: A Systematic Review. *J. Appl. Sci. Environ. Manage.* 28 (4) 1129-1150

Dates: Received: 22 January 2024; Revised: 29 February 2024; Accepted: 23 March 2024 Published: 29 April 2024

Keywords: Dosimeter; radiation, thermoluminescence, thermoluminescence applications

Thermoluminescence was first observed in 1663 by the Dutch physicist Nicolas Steno, who noticed that some minerals emit light when heated. However, until the 1930s, TL began to be studied systematically; in

*Corresponding Author Email: godwin.efenji@fulokoja.edu.ng

*ORCID: <https://orcid.org/0000/0002/14262111>

*Tel: +2347067022609

1938, the French physicist Jean Perrin discovered that certain minerals could be used to measure radiation exposure, and in 1947, the American physicist Farrington Daniels developed the first TL dosimeter (Murthy, 2014). Since then, TL has been used in various applications, including dating archaeological materials, dosimetry, and detecting radiation. The development of TL materials has been an essential part of this progress, as materials with improved TL properties have allowed for more precise TLD materials to play a crucial role in this technique, as they are responsible for the storage and release of energy that can be measured and correlated to the absorbed dose. The structural properties of TLD materials, such as crystal structure, defects, impurities, and dopants, can significantly affect their thermoluminescence properties and overall dosimetric performance. Therefore, a comprehensive understanding of the structural properties of TLD materials is essential to optimise their performance and reliability for radiation dosimetry applications (Bengisu, 2016). Furthermore, this review discusses the adaptability of TLD materials for different dosimetry applications, such as personal Dosimetry, environmental Dosimetry, Medical Dosimetry, and space Dosimetry. It examines the specific requirements of each application and how other TLD materials can meet these requirements (Osama *et al.*, 2020). The information presented in this review is drawn from a broad range of literature sources, including research articles, review papers, and conference proceedings. The references used in this review are selected based on their relevance, significance, and reliability. Overall, this review provides a comprehensive and up-to-date understanding of the structural properties of TLD materials, their preparation methods, and their adaptability for different dosimetry applications (Efenji *et al.*, 2023; Jamil *et al.*, 2023). The crystal structure of TLD materials, particularly LiF and CaF₂, is crucial in determining their thermoluminescence properties. For example, LiF has a face-centred cubic structure that exhibits high sensitivity to ionising radiation and low fading rates. In contrast, CaF₂ has a fluorite structure, resulting in lower sensitivity but higher energy resolution (El-Egili and Oraby, 1996). TLD materials defects, impurities, and dopants can significantly affect their thermoluminescence properties. For example, lithium interstitials in LiF can enhance thermoluminescence efficiency, while contaminants such as carbon and oxygen can reduce the efficiency. Dopants such as magnesium and manganese can modify the thermoluminescence properties of TLD materials and enhance their sensitivity to ionising radiation (El-Faramawy *et al.*, 2021a). Several methods can be used to prepare TLD

materials, including solid-state synthesis, solution-based methods, and thin film deposition techniques. Solid-state synthesis methods involve high-temperature treatments of precursor materials to form TLD materials, while solution-based methods involve the precipitation of TLD materials from solutions containing precursor salts. Thin film deposition techniques such as pulsed laser deposition and electron beam evaporation fabricate TLD materials with controlled thickness and morphology (Saidu *et al.*, 2015).

The adaptability of TLD materials for different dosimetry applications is primarily determined by their thermoluminescence properties, sensitivity, energy resolution, and fading rates. For example, TLD-100 is widely used in medical dosimetry due to its high sensitivity and energy resolution. At the same time, LiF is preferred for personal dosimetry applications due to its low fading rate and increased sensitivity to low-energy radiation. Other TLD materials, such as CaF₂ and Li₂B₄O₇, are suitable for environmental and space dosimetry applications (Pal *et al.*, 2011).

The structural properties of TLD materials play a significant role in their thermoluminescence properties and overall dosimetric performance. Understanding these properties and their effects on TLD materials can optimise their performance and reliability for different dosimetry applications. This review provides a comprehensive overview of the structural properties of TLD materials, their preparation methods, and their adaptability for various dosimetry applications. It is a valuable resource for researchers and practitioners in radiation dosimetry, measurements, and more diverse applications (Murthy, 2014).

This review aims to provide a comprehensive overview of the structural properties of TLD materials, their preparation methods, and their adaptability for different dosimetry applications. It begins with a brief introduction to the principles of thermoluminescence and the essential characteristics of TLD materials. Subsequently, it discusses the various structural properties of TLD materials, including their crystal structure, defects, impurities, and dopants, and their effects on thermoluminescence properties. It also covers the different methods of preparing TLD materials, including solid-state synthesis, solution-based methods, and thin film deposition techniques, and their advantages and limitations (K and Reddy, 2008)

Basics structural properties of TLD materials

Efenji, G. I; ISKANDAR, S. M; YUSOF, N. N; RABBA, J. A; MUSTAPHA, O. I; FADHIRUL, I. M; UMAR, S. A; KAMGBA, F. A; USHIE, P. O; MUNIRAH, J; THAIR, H. K; NABASU, S. E; HAYDER, S. N OKE, A O.

Defects in the crystal lattice of TLD materials: Thermoluminescent dosimeter (TLD) materials are frequently employed in radiation dosimetry to assess the radiation dosage received by matter or human tissue. The crystal structure of these materials contains flaws that can trap electrons or holes produced by ionising radiation (*El-Faramawy et al., 2021a*). The following are the most typical flaws with TLD materials:

F-centres are electron traps produced by an anion vacancy in the crystal lattice. An anion vacancy results from a missing negative ion in the lattice, which generates an excess positive charge. Thermal or visual stimulation can excite the trapped electron to a higher energy level, producing light emission.

H-centres: The cation vacancy in the crystal lattice causes these hole traps to form. A missing positive ion produces an extra negative charge called a "cation vacancy" in the lattice. Light is emitted when the trapped hole is stimulated thermally or optically to a higher energy level.

Colour centres: These are flaws brought about by dopants or impurities in the crystal lattice. These defects may function as electron or hole traps depending on the kind of dopant or impurity present. Light can be emitted when colour centres are stimulated thermally or optically to more incredible energy.

Generally, the ability of TLD materials to capture and release electrons or holes produced by ionising radiation depends critically on flaws in their crystal lattice. As the TLD material is heated, the flaws serve as the source of luminescent centres that produce light, enabling the measurement of the radiation dose (*Duragkar et al., 2019*).

Deep-level traps of TLD materials: Deep-level traps that can capture electrons or holes produced by ionising radiation are another feature of thermoluminescent dosimeter (TLD) materials in addition to crystal lattice defects. Impurities or flaws in the crystal lattice that build localised energy states within the material bandgap often cause these traps to form. Deep-level traps in TLD materials frequently take the following forms:

Traps produced by transition metal ions: TLD materials may contain deep-level traps from transition metal ions like copper (Cu) and manganese (Mn). These traps are frequently produced when a transition metal ion is found where the crystal lattice has a lower symmetry.

Rare earth ion-produced traps: Europium (Eu) and Cerium (Ce) rare earth ions can produce deep-level traps in TLD materials. These traps are often made when a rare earth ion is found where the crystal lattice has less symmetry.

Traps caused by crystal lattice flaws: In TLD materials, imperfections in the crystal lattice, such as vacancies and dislocations, can produce deep-level traps. Localised energy levels inside the material bandgap frequently result in the formation of these traps.

Deep-level traps should be present for TLD materials to capture and release electrons or holes produced by ionising radiation. When a TLD material is heated, trapped electrons or holes may be thermally released from deep-level traps, which causes light to be emitted. This light can be monitored to quantify the radiation dose the material receives (*Pekpak et al., 2014*).

Electronic structure of TLD materials: Materials for thermoluminescent dosimeters (TLD) can display thermoluminescence due to the large part of their electrical structure. The band gap between the two bands determines the energy needed to excite electrons from the valence band to the conduction band in TLD materials. TLD materials can have the following characteristics because of their electrical structure:

Formation of electron-hole pairs: When TLD materials are subjected to ionising radiation, the energy of the radiation can excite electrons from the valence band to the conduction band, forming electron-hole pairs. Trapping of excited electrons or holes: TLD materials have flaws or imperfections in their crystal lattice that allow them to capture excited electrons or holes produced by ionising radiation. Both deep-level and shallow-level traps are possible. Thermal ejection of trapped electrons or holes from the traps: When a TLD material is heated, trapped electrons or holes can thermally eject themselves from the traps, regaining their initial energy and releasing it as light. Light emission: The trapped electrons or holes release energy in the form of light, which may be monitored to establish how much radiation the TLD material has been exposed to.

Generally, the capacity of TLD materials to capture, display thermoluminescence, and release electrons or holes produced by ionising radiation depends critically on their electrical structure. Designing and improving TLD materials for various radiation dosimetry applications requires understanding their electrical structure (*El-Faramawy et al., 2021a*).

Table 1. The physical structure of some TLD materials advantages, disadvantages, and recommendations.

S/N	Physical Structure	Advantages	Disadvantages	Recommendation	Reference
1	Al ₂ O ₃ :C	High sensitivity and reproducibility	Low thermal stability	Good for dosimetry and dating applications	(Pal et al., 2011), (Rao et al., 2002)
2	MgB ₄ O ₇ :Dy	High TL intensity and sensitivity	Low thermal stability and fading	Suitable for high-dose Dosimetry	
3	CaSO ₄ :Dy	High sensitivity and reproducibility	Low thermal stability and fading	Suitable for low to medium-dose Dosimetry	(El-Faramawy et al., 2021a), (Lim et al., 2015; Prabhu et al., 2021)
4	LiF: Mg, Ti	High sensitivity and reproducibility	Low thermal stability and fading	Good for personal Dosimetry	
5	Li ₂ B ₄ O ₇ : Mn	High TL intensity and sensitivity	Low thermal stability and fading	Suitable for high-dose Dosimetry	(Pekpak et al., 2014), (Rivera, 2012; Singh and Kainth, 2018)
6	KBr: Eu	High TL intensity and sensitivity	Low thermal stability and fading	Suitable for high-dose Dosimetry	
7	NaCl: Tl	High sensitivity and reproducibility	Low thermal stability and fading	Suitable for personal dosimetry	(Bootjomchai and Laopaiboon, 2014), (Saidu et al., 2015)
8	LiF: Mg, Cu, P	High sensitivity and reproducibility	Low thermal stability and fading	Good for personal Dosimetry	
9	MgO: Mn	High TL intensity and sensitivity	Low thermal stability and fading	Suitable for high-dose Dosimetry	(Ravikumar et al., 2018), (Duragkar et al., 2019)
10	CaSO ₄ :Mn	High sensitivity and reproducibility	Low thermal stability and fading	Suitable for low to medium-dose Dosimetry	
11	BaFCl: Eu	High TL intensity and sensitivity	Low thermal stability and fading	Suitable for high-dose Dosimetry	
12	LiF: Mg, Cu, P, Ag	High sensitivity and reproducibility	Low thermal stability and fading	Good for personal Dosimetry	
13	LiF: Cu, P	High sensitivity and reproducibility	Low thermal stability and fading	Suitable for personal Dosimetry	
14	CaSO ₄ :Tm	High sensitivity and reproducibility	Low thermal stability and fading	Suitable for low to medium-dose dosimetry	(McKeever, 1997), (Bootjomchai and Laopaiboon, 2014; Salama and Soliman, 2018)
15	BaFBr: Eu	High TL intensity and sensitivity	Low thermal stability and fading	Suitable for high-dose Dosimetry	
16	CaSO ₄ :Eu	High sensitivity and reproducibility	Low thermal stability and fading	Suitable for low to medium-dose dosimetry	(Hashim et al., 2014), (Kawamura et al., 2020)
17	Al ₂ O ₃ :C,Mg	High sensitivity and reproducibility	Low thermal stability	Good for dosimetry and dating applications	
18	CaF ₂ :Mn	High TL intensity and sensitivity	Low thermal stability and fading	Suitable for high-dose Dosimetry	(Aydin et al., 2013), (Mishra et al., 2016; Razak et al., 2016)
19	KCl: Eu	High sensitivity and reproducibility	Low thermal stability and fading	Suitable for high-dose Dosimetry	
20	LiF:Mg,Cu,Na,Si	High sensitivity and reproducibility	Low thermal stability and fading	Good for personal dosimetry	

The best physical structure for a specific application depends on the particular needs and requirements (El-Adawy et al., 2010). However, based on the summarised advantages and disadvantages of the physical structures listed in Table 1, the following are some recommendations:

For dosimetry and dating applications, Al₂O₃:C or Al₂O₃:C, Mg are good choices due to their high sensitivity and reproducibility. For personal Dosimetry, LiF: Mg, Ti, LiF: Mg, Cu, P, or LiF: Cu, P are suitable options due to their high sensitivity and reproducibility. For low to medium dose dosimetry, CaSO₄:Dy, CaSO₄:Mn, CaSO₄:Tm, or CaSO₄:Eu are recommended due to their high sensitivity and reproducibility. For high-dose Dosimetry, MgB₄O₇:Dy, Li₂B₄O₇:Mn, KBr: Eu, MgO: Mn,

BaFCl: Eu, BaFBr: Eu, CaF₂:Mn, or KCl: Eu are good choices due to their high TL intensity and sensitivity. Choosing the best physical structure for a specific application depends on the particular needs and requirements and careful consideration of the advantages and disadvantages of each option before making a final decision (Pal et al., 2011).

Stability of luminescence centre of TLD materials: The reliability and accuracy of thermoluminescent dosimeter (TLD) materials in radiation dosimetry are significantly influenced by the stability of the luminescent centre (Stanković Petrović et al., 2021). The crystal structure of TLD materials can have imperfections or impurities that can produce luminescent centres. These centres can become unstable under specific circumstances, reducing the

sensitivity or accuracy of radiation measurements. The following elements can have an impact on the stability of luminous centres in TLD materials:

Temperature: In TLD materials, high temperatures may damage the luminous centres, resulting in centre migration or destruction. As a result, radiation readings may become less sensitive or accurate.

Radiation exposure: Ionising radiation exposure has the potential to have an impact on the luminescent centres in TLD materials. A decrease in sensitivity or accuracy in radiation measurements can result from

high radiation doses damaging the material crystal lattice.

Chemical environment: The Stability of the luminous centre can also be impacted by the chemical environment of the TLD material. The luminous centre may alter or disappear after exposure to specific chemicals or gases (*Hamzah et al., 2017*).

Ageing: Due to normal ageing processes, the luminous centres in TLD materials may deteriorate or change over time. Radiation measurements may become less sensitive or accurate because of this.

Table 2. Stability of luminescence centres for TLD materials

TLD Material	Luminescence Centre	Stability	Reference
LiF: Mg, Ti	F centre	Stable	<i>(Godwin et al., 2023), (Kaur et al., 2017)</i>
	F2 centre	Unstable	
	F3 centre	Unstable	
LiF: Mg, Cu, P	F centre	Stable	<i>(Pekpak et al., 2014), (Himamaheswara Rao et al., 2018)</i>
	F2 centre	Unstable	
	F3 centre	Unstable	
	Cu centre	Stable	
	P centre	Stable	
CaSO4:Dy	SO4 centre	Stable	<i>(Pal et al., 2011)</i>
	Dy centre	Stable	
Al2O3:C	ODC	Stable	<i>(El-Adawy et al., 2010), (Babu et al., 2011)</i>
	NV centre	Stable	
MgO: Ni, Ti	Ti centre	Stable	<i>(Duragkar et al., 2019)</i>
	Ni centre	Stable	
	Ti-Ni centre	Stable	
KCl: Tl	Tl centre	Stable	<i>(Jaidass et al., 2018)</i>
	F centre	Stable	
	H centre	Stable	
	K centre	Stable	
Li2B4O7:Cu,P	Cu centre	Stable	<i>(Bengisu, 2016), (Ravikumar et al., 2018)</i>
	P centre	Stable	
	F centre	Unstable	
	F2 centre	Unstable	
	F3 centre	Unstable	
SrB4O7:Eu	Eu centre	Stable	<i>(Stanković Petrović et al., 2021)</i>
Li2B4O7:Cu,P	Cu centre	Stable	
	P centre	Stable	
	F centre	Unstable	
	F2 centre	Unstable	
	F3 centre	Unstable	
SrB4O7:Eu	Eu centre	Stable	<i>(Ike et al., 2021), (Pawar et al., 2017)</i>
Li2B4O7:Cu,P	Cu centre	Stable	
	P centre	Stable	
	F centre	Unstable	

Table 2 shows the stability of luminescence centres for TLD materials. The stability of luminescence centres refers to the ability of the excited electrons to remain in their excited state until they are heated and release their energy. If the luminescence centres are unstable, they can decay before being read by the TLD reader, leading to inaccurate dose measurements. Therefore, the stability of luminescence centres is a crucial factor in determining the accuracy of TLD dosimetry.

Several factors can affect the stability of luminescence centres, including the purity of the TLD material, the concentration and type of dopants, and the annealing temperature and time. Different TLD materials have different stability characteristics, and some may be more prone to instability than others (*El-Adawy et al., 2010*). In general, TLD materials with high stability of luminescence centres are preferred in dosimetry applications to ensure accurate and reliable dose

measurements. Unstable luminescence centres can lead to significant errors in dose measurements, which can have severe consequences in medical, industrial, or environmental settings. It is crucial to store and treat TLD materials carefully, keep them away from extreme heat and radiation, and test them occasionally to ensure they are working correctly to preserve the stability of the luminous core (Rao et al., 2002).

Sensitivity of TLD materials: The ability of TLD materials to recognise and react to low doses of ionising radiation is referred to as their sensitivity. The following variables can influence how sensitive TLD materials with the table 3:

Composition: The susceptibility of TLD materials to ionising radiation might vary according to their chemical makeup. Lithium fluoride (LiF) is an example of a material with a more significant atomic number than calcium fluoride, making it more sensitive to ionising radiation (CaF₂).

Impurities and flaws: In the crystal lattice of TLD materials, imperfections and flaws can result in luminous centres sensitive to ionising radiation. The concentration and distribution of these impurities and flaws may impact the sensitivity of the TLD material.

Annealing and processing conditions: The sensitivity of TLD materials might be impacted by the annealing and processing procedures utilised during production. The concentration and distribution of luminous centres in the material can change depending on the temperature, time, and environment employed during annealing.

Reading conditions: The sensitivity of TLD materials can also be impacted by the reading circumstances employed to test their thermoluminescent response. Variables, including heating rate, heating time, and temperature range, can influence the sensitivity of the material (Saidu et al., 2018).

Table 3. TLD materials and sensitivity

TLD Material	Sensitivity	Reason for Sensitivity	Reference
LiF: Mg, Ti	High	The high density of traps and efficient trapping of electrons and holes.	(Stanković Petrović et al., 2021), (Hashim et al., 2014; Pawar et al., 2017)
LiF: Mg, Cu, P	Medium-high	The high density of traps and efficient trapping of electrons and holes, but lower sensitivity compared to LiF: Mg, Ti due to Cu and P impurities.	
CaSO ₄ :Dy	Medium	The lower density of traps and lower efficiency in trapping electrons and holes compared to LiF-based TLDs are still relatively sensitive.	
Li ₂ B ₄ O ₇ :Cu,P	Medium	The lower density of traps and lower efficiency in trapping electrons and holes compared to LiF-based TLDs are still relatively sensitive.	(Bengisu, 2016), (Boottjomchai & Laopaiboon, 2014; Hashim et al., 2014)
LiF: Mg, Cu	Medium	Lower sensitivity compared to LiF: Mg, Ti due to the absence of Ti impurities, which are known to enhance sensitivity.	
Mg ₂ SiO ₄ :Mn	Low-medium	The lower density of traps and lower efficiency in trapping electrons and holes than LiF-based TLDs lead to lower sensitivity.	

The composition and production methods used to create TLD materials must be carefully chosen and optimised to maximise their sensitivity. The reading circumstances should also be thoroughly controlled and standardised to provide precise and consistent measurements of ionising radiation doses. Furthermore, the TLD materials' sensitivity and accuracy in radiation dosimetry can be enhanced by calibrating them with a known radiation source (Godwin et al., 2023)

Fading of TLD materials: The thermoluminescent signal from previously irradiated thermoluminescent dosimeter (TLD) materials fades with time, even without any radiation exposure, according to a phenomenon known as fading. Due to the possibility of inaccurate radiation dose assessments, this presents

a significant challenge for radiation dosimetry. The fading of TLD materials is a result of a variety of factors, including the following:

Trap emptying: In TLD materials, fading may happen because trapped electrons or holes are thermally released from the luminous centres. The trapped electrons or holes may eventually thermally escape from their traps, which would reduce the luminous signal over time.

Radiation-induced modifications: The crystal lattice of TLD materials can undergo radiation-induced changes that can result in fading. The luminous signal may gradually weaken because radiation exposure alters the luminescent centres or produces new ones.

EFENJI, G. I; ISKANDAR, S. M; YUSOF, N. N; RABBA, J. A; MUSTAPHA, O. I; FADHIRUL, I. M; UMAR, S. A; KAMGBA, F. A; USHIE, P. O; MUNIRAH, J; THAIR, H. K; NABASU, S. E; HAYDER, S. N OKE, A O.

Storage conditions: How TLD materials are stored can impact how quickly they deteriorate. Exposure to high temperatures or humidity can speed up the fading process (Pal *et al.*, 2011).

In general, the fading of TLD materials (Table 4) occurs when the trapped electrons and holes responsible for the TL signal are released from their traps due to various external factors. Thermal annealing, phototransfer, or other forms of electronic trapping may be the cause of this. The TL signal may gradually decline because of fading, which may impact the measurement's accuracy. On the other hand, non-fading TLD materials can retain their TL signal over time due to their structural stability or electronic trapping mechanisms. These materials are typically more reliable for TL dosimetry applications (El-Faramawy *et al.*, 2021a).

Several different actions can lessen the effects of fading in TLD materials. The TLD materials should be kept in ideal storage conditions to minimise any impact from storage. Moreover, the TLD material's pre-irradiation annealing can lessen fading effects. The TLD material must be heated to a high temperature to empty the traps and stabilise the luminous centres before radiation exposure (Singh & Kainth, 2018). Correction factors apply to the measurements acquired from TLD materials to account for fading effects. The dose measurements received from the TLD material can be adjusted using these correction factors, which are developed by tracking the fading characteristics of the TLD material over time (Stanković Petrović *et al.*, 2021).

Table 4. Fading of some TLD materials and reasons for fading or non-fading

TLD Material	Fading or Non-Fading	Reason for Fading	Reason for Non-Fading	Reference
LiF: Mg, Ti	Fading	Thermal annealing	Electronic trapping	(Ab Rasid <i>et al.</i> , 2015)
LiF: Mg, Cu, P	Non-Fading	-	Electronic trapping	(Pawar <i>et al.</i> , 2017)
CaSO ₄ :Dy	Fading	Phototransfer	Electronic trapping	
Li ₂ B ₄ O ₇ :Cu,P	Non-Fading	-	Structural Stability	(El-Faramawy <i>et al.</i> , 2021a), (Sanyal <i>et al.</i> , 2019)
MgB ₄ O ₇ :Dy	Fading	Phototransfer	Electronic trapping	
Al ₂ O ₃ :C	Non-Fading	-	Structural Stability	
LiF: Mg, Ti	Fading	Thermal annealing	Electronic trapping	

Preparation of TLD materials: Ionising radiation dosage is measured using thermoluminescence (TL) Dosimetry. The response of TL materials to ionising radiation is observed by heating the materials to cause the trapped charges to escape. The procedures for getting TL materials ready for dosimetry are as follows:

Choosing the suitable materials: TL materials should have a high TL efficiency, increased sensitivity to ionising radiation, and low TL signal fading over time. LiF, MgF₂, CaF₂, and TLD-100 are some of the more popular TL materials.

Purification: The chosen TL material needs to be cleaned to eliminate any contaminants that could impede the TL reaction. Re-crystallisation, sublimation, and zone melting are purification processes.

Preparation of the material: To create pellets or discs, the TL material is ground into a fine powder and combined with a binder. The binder should be chemically inert and not alter the material's TL response. PTFE (polytetrafluoroethylene), epoxy, and

paraffin are often used as binders. Fabrication of TL dosimeters: After being combined with the binder, the TL material is pressed into an appropriate shape, like a disc or a rod. Afterwards, any remaining tensions in the material are eliminated by annealing the dosimeters. Calibration: A calibrated radiation source, such as a Cs-137 or Co-60 source, calibrates the TL dosimeters. A calibration factor is calculated after determining the dosimeter dose-response.

Storage: The TL dosimeters should be handled carefully to prevent damage and stored in a dry, excellent location away from radiation sources (Lim *et al.*, 2015; Prabhu *et al.*, 2021).

As seen in table 5, the choice of preparation method depends on the specific application and the desired properties of the TLD material. Solid-state sintering and sol-gel techniques are generally preferred for high-quality dosimetry, while chemical precipitation may be sufficient for lower-quality applications. It is essential to carefully consider the advantages and disadvantages of each method and choose the appropriate technique to achieve accurate and reliable Dosimetry (Mhareb *et al.*, 2016).

EFENJI, G. I; ISKANDAR, S. M; YUSOF, N. N; RABBA, J. A; MUSTAPHA, O. I; FADHIRUL, I. M; UMAR, S. A; KAMGBA, F. A; USHIE, P. O; MUNIRAH, J; THAIR, H. K; NABASU, S. E; HAYDER, S. N OKE, A O.

Table 5. Methods of preparation of TLD materials for thermoluminescence advantages, disadvantages, and recommendations.

Method of preparation	Advantages	Disadvantages	Recommendation	Reference
Solid-State Reaction	Simple, high purity	Prolonged reaction time, high sintering temperature	Suitable for large-scale production	(Sundaraman <i>et al.</i> , 2020), (Sanyal <i>et al.</i> , 2019; Thomas <i>et al.</i> , 2019)
Sol-Gel Method	Controlled composition and morphology, low temperature	High pressure and temperature, complex process	Ideal for preparing complex oxides and nanomaterials	
Co-precipitation Method	Homogeneous mixing, easy control of dopant concentration	Potential impurities, limited composition range	Suitable for preparing highly doped materials	
Hydrothermal Synthesis	High purity, controlled morphology	High pressure and temperature, complex process	Suitable for preparing complex oxides and nanomaterials	(Murthy, 2014), (Hashim <i>et al.</i> , 2017; Thomas <i>et al.</i> , 2019)
Microwave Synthesis	Fast reaction time, energy-efficient	Limited to small batches, potential inhomogeneity	Suitable for preparing small quantities of materials	
Electrospinning	Controlled morphology, high surface area	Limited to specific materials, potential defects	Suitable for preparing nanofibers and composites	
Spray Pyrolysis	Uniform coatings, low cost	Limited to specific materials, potential defects	Suitable for preparing thin films	
Plasma Spray	High deposition rate, controlled porosity	High temperature, limited to specific materials	Suitable for preparing coatings and porous materials	
Chemical Vapor Deposition	Controlled deposition, high purity	High temperature, limited to specific materials	Suitable for preparing thin films	
Hydrogen Reduction	Simple, low-cost	Limited to specific materials, potential impurities	Suitable for preparing oxide materials	
Combustion Synthesis	Fast reaction time, low cost	Limited to specific materials, potential impurities	Suitable for preparing complex oxides	(Bengisu, 2016), (Hashim <i>et al.</i> , 2017)
Sintering	High-density, simple	Limited to specific materials, potential defects	Suitable for preparing dense materials	
Hydrogen Peroxide Synthesis	Controlled composition, low temperature	Limited to specific materials, potential impurities	Suitable for preparing oxide materials	
Solvothermal Synthesis	High purity, controlled morphology	High pressure and temperature, complex process	Suitable for preparing complex oxides and nanomaterials	
Ion Implantation	Controlled doping, high purity	Complex process, limited to specific materials	Suitable for preparing highly doped materials	
Pulsed Laser Deposition	Controlled deposition, high purity	Expensive equipment, limited to specific materials	Suitable for preparing thin films	
Ball Milling	Homogeneous mixing, controlled particle size	Limited to specific materials, potential defects	Suitable for preparing powders and composites	
Freeze-Drying	Controlled morphology, low temperature	Limited to specific materials, potential defects	Suitable for preparing porous materials and composites	
Mechanochemistry	Simple, low-cost	Limited to specific materials, potential defects	Suitable for preparing powders and composites	
Chemical Bath Deposition	Controlled deposition, low cost	Limited to specific materials, potential defects	Suitable for preparing thin films	
Solvent Assisted Grinding	Simple, low-cost, eco-friendly	Limited to specific materials, potential defects	Suitable for preparing powders and composites	(Stanković Petrović <i>et al.</i> , 2021), (Thomas & Chithambo, 2017), (Bradley <i>et al.</i> , 2020; Sani <i>et al.</i> , 2020)
Ultrasonic Spray Pyrolysis	High uniformity, low cost	Limited to particular materials, possible defects	Ideal for preparing thin films	
Hydrothermal Decomposition	Controlled morphology, low temperature	Limited to specific materials, potential defects	Suitable for preparing nanoparticles	
Chemical Precipitation	Low cost, easy scale-up	Potential impurities, limited composition range	Suitable for preparing powders and composites	(Pal <i>et al.</i> , 2011)
In-situ Polymerization	Controlled morphology, low cost	Limited to certain materials	----	
Melt Quenching	Simple, high-purity	Limited to specific materials, potential defects	Suitable for preparing glasses and amorphous materials	(Ichoja <i>et al.</i> , 2018), (Khazaalah <i>et al.</i> , 2022)
Electrodeposition	Controlled deposition, high purity	Limited to specific materials, potential defects	Ideal for preparing coatings and composites	

Evaluation methods: All techniques rely on the straightforward TL model, which posits that radiation results in the production of free electrons, which results in the creation of energy levels in the forbidden

band. The two most crucial variables that must be analysed in relation to the trap levels are the frequency factors and the trap depth E , or the amount of thermal energy required to release the trapped electrons

EFENJI, G. I; ISKANDAR, S. M; YUSOF, N. N; RABBA, J. A; MUSTAPHA, O. I; FADHIRUL, I. M; UMAR, S. A; KAMGBA, F. A; USHIE, P. O; MUNIRAH, J; THAIR, H. K; NABASU, S. E; HAYDER, S. N OKE, A O.

(Azorín et al., 1993). As seen in equation (1), the first ascent method is based on studies of the low-temperature side of TL peaks, where it is possible to assume that the number of trapped electrons is constant, allowing for a good approximation of the temperature dependency of the TL signal (Efenji et al., 2023; K et al., 2017).

$$I(T) \propto e^{(-E/kT)} \quad (1)$$

Under this assumption, the t_{4e} value of E can be calculated by graphing $\ln I(T)$ vs $1/T$. However, some authors like AK Singhvi, et al., 2011, stated that this approach has numerous shortcomings.

Various heating rates: The TL peak's maximum temperature (TM) varies as the heating rate changes, and an increase in the heating rate causes the peak to shift to higher values of Tw. A first-order kinetics technique using two variables was proposed to use heating rates using this characteristic. The following mathematical relationship can be used to calculate E:

$$E = k \frac{T_{m1}T_{m2}}{T_{m1}-T_{m2}} \ln \left[\frac{\beta_1}{\beta_2} \left(\frac{T_{m1}}{T_{m2}} \right)^2 \right] \quad (2)$$

Similar formulas are constructed for the kinetics of additional orders (Reddy, 2012). The following are the frequency factors:

$$s = \frac{\beta E}{kT_m^2} e^{\left(\frac{E}{kT_m} \right)} \quad (3)$$

Suppose a steady temperature is maintained for the TL sample after stimulation, and the light emission is recorded as a function of time. In that case, the reduction process of the trapped electrons can be identified using the isothermal decay approach. The following equation for first-order kinetics can be used to evaluate the decay curve produced for a particular storage temperature T:

$$I(t) = \frac{n_0}{\tau} e^{\left(\frac{-t}{\tau} \right)} \quad (4)$$

Where $\tau = e^{\left(\frac{E}{kT} \right)}$

Peak shape method: The standard TL peak parameters, which determine the luminous peak halfwidth and include the temperature values TI, T, and the maximum temperature TM., are utilised in several methods. Different ways of expressing first- and second-order kinetics were used (Reddy, 2012). the geometrical factor $Ps = \frac{(T-TM)}{(Tz-TI)}$, which ranges between 0.42 and 0.52, was used to generate the

following set of equations (14) for computing E, regardless of the kinetics order.

$$E_\alpha = c_\alpha \left(k \frac{T_m^2}{\alpha} \right) - b_\alpha (2kT_m) \quad (5)$$

Based on the advantages and disadvantages listed in Table 2, the best preparation method for thermoluminescence materials will depend on the application's specific needs. However, some general considerations can be made. For example, solid-state reaction and sol-gel methods suit large-scale production and preparation of thin films and composites. Co-precipitation is ideal for highly doped materials, while hydrogen reduction is simple and low-cost but limited to certain materials. Ball milling is suitable for preparing powders and composites, while melt quenching is ideal for amorphous materials (Aloraini et al., 2022).

In general, the choice of preparation method will depend on factors such as the desired composition, morphology, and purity of the material and the specific application. It is recommended to consult an expert in thermoluminescence materials to determine the most appropriate method for a given application (Saidu et al., 2018).

Luminescence Fundamentals: Light is emitted by a substance when it takes in external energy, such as ultraviolet radiation. This process is known as luminescence. The emission can be classified as either luminescence or fluorescence, depending on the expected duration between excitation energy absorption and luminescence emission (Furetta et al., 2001). The process is easily categorised as fluorescence for light emission with 10-8s; however, when $T >$ a few seconds. The activity is phosphorescence. The best approach to distinguish between the two procedures is to use the temperature dependency of T, which is not always apparent in between. Consider the ground state energy level g in Figure (1a) and the excited state energy level e. (a) when an electron is excited from state g to state e and then returns to state g, it emits light, referred to as fluorescence. If the transfer is spin- or parity-banned, A few milliseconds is all that an enthusiastic mood can last. Take the d-electron in the Mn²⁺ ions in the thermoluminescent phosphor CaF₂: Mn, for example, a transition from the ground state to the first excited state of 4Ti₉ (4G) under light absorption. The lifetime of an excited state electron is $T \ll 5$ Ms before it returns to the ground state and emits a photon with an $\lambda = 500$ nm wavelength (Kawamura et al., 2020).

Efenji, G. I; ISKANDAR, S. M; YUSOF, N. N; RABBA, J. A; MUSTAPHA, O. I; FADHIRUL, I. M; UMAR, S. A; KAMGBA, F. A; USHIE, P. O; MUNIRAH, J; THAIR, H. K; NABASU, S. E; HAYDER, S. N OKE, A O.

However, excitation and emission can have much longer delays if a transit delays the transition to the initial condition into and out of a metastable level *m*, a condition known as phosphorescence figure 1(b). Suppose the transition into level *m* occurs at a temperature *T* such that the energy *E* of separation between *m* and *e* is $E > \text{many } kT$ (*k* is Boltzmann's constant). The electron is anticipated to stay at level *m* long (Murthy, 2014). In this case, the probability *p* per unit time of thermal stimulation from the trap, taking into account a Maxwellian arrangement of energy, is proportional to temperature, as demonstrated by equation (6) (Azorín et al., 1993)

$$P = se^{\{-E/kT\}} \tag{6}$$

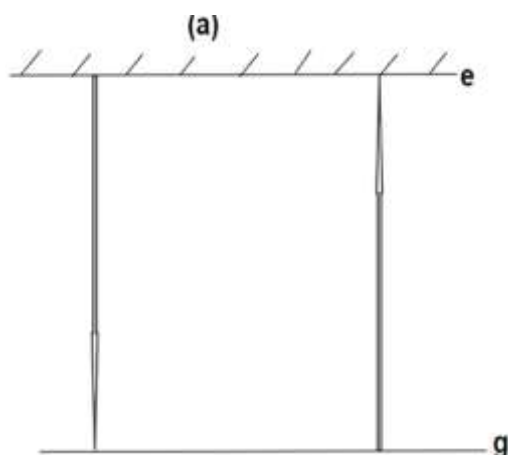


Fig. 1a: Illustration of fluorescence absorption at excite and ground state energy levels

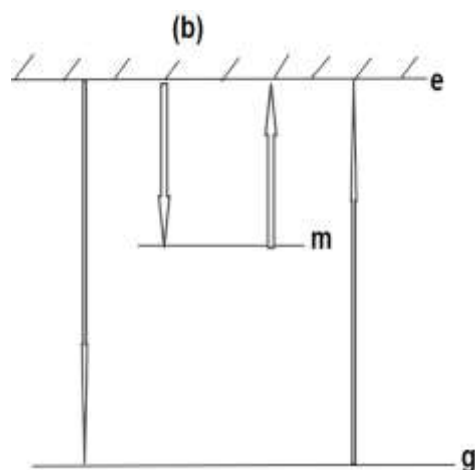


Fig. 1b: Excitation and emission delayed by metastable level *m* during phosphorescence

Consequently, because the electron is present in the metastable state, excitation and ultimate relaxation returning to the ground state take longer, where *s* is a constant with reciprocal time dimensions. Such a process would be temperature sensitive due to the

exponential function in equation (1), allowing one to distinguish between the phosphorescence process, which is highly temperature dependent, and the fluorescence process, which is just somewhat temperature dependent. The differentiating characteristic is in the existence of the metastable stage *m*. The name of the luminescence phenomenon depends on the energy used for excitation before the emission begins (Salah, 2011). Thus, the absorption of electron beams creates cathodoluminescence, the absorption of nuclear power causes radioluminescence, and light absorption causes photoluminescence, usually UV or visible from gamma rays, x-rays, etc (Ichoja et al., 2018). Additionally, luminescence is triggered by various energies, including sound wave energy, mechanical energy, electrical energy, and electroluminescence (sonoluminescence). Any of these situations can result in an emission that happens immediately from an ecstatic mood or is postponed by a metastable state (Bengisu, 2016). In this regard, it is essential to point out that the term thermoluminescence is misleading since heat is not the primary excitation source in contrast to the previous examples. Since heat only stimulates emission rather than excitation, the more accurate term thermally stimulated luminescence (TSL) for phosphorescence is commonly used instead of TL. However, in all its uses, the word thermoluminescence is now frequently employed (L.A. Owen, U. Kampb, J. Q. Spencer, 2002; Murthy, 2014).

Phosphorescence: The metastable energy level must be involved in comprehending the phenomena in the processes discussed and explored in this review. The lifespan at this level, whose temperature dependence is given by equation (2), can be any value up to the material's age if the temperature *T* is low enough and the activation energy *E* is high enough to slow the thermal emission rate. After the excitation has ended, let's say at any random time, when there is an electron concentration of *n* in level *m*. The rate of thermal excitation of electrons from level *m* to *e*, according to Duragkar et al. (2019), is.

$$-\frac{dn}{dt} = np = nse^{\{-E/kT\}} \tag{7}$$

When the negative sign indicates electron loss in the absence of re-trapping, the frequency of *m*→*e* transitions control the intensity *I* of the luminescence brought on by the electron decay from the excited state *e* to the ground state *g*, leading to

$$I(t) = -\eta \frac{dn}{dt} = \eta nse^{\{-E/kT\}} \tag{8}$$

Where η is a constant. Integration yields

$$I(t) = I_0 e^{\{-tp\}} \quad (9)$$

Where $I(t)$ denote the intensity's beginning at time $t = 0$. Thus, the decrease in phosphorescence at a constant temperature is a simple exponential function of time. The residence period in the metastable state grows incredibly long if $E > kT$, suggesting that the electrons in m can last forever. For instance, at 298 K, $p = 7.3 \times 10^5$ years if $E = 1.5$ eV and $s = 1012$ s. It's common to observe decays that go beyond a simple exponential. Randall and Wilkins also consider the possibility of having an equal likelihood that the excited electron will be re-trapped in level m or recombined in level g . (later Garlick and Gibson). Under these conditions, Eq. (8) becomes.

$$I(t) = -\eta \frac{dn}{dt} = \alpha n^2 \quad (10)$$

Where α is a fixed value at constant Integration of T . now produces

$$I(t) = \frac{I_0}{(n_0 \alpha t + 1)^2} \quad (11)$$

Since the decay rate in Equations 8 and 9 is proportional to n , we obtain a first workflow. On the other hand, in equation (10), the decay rate is proportional to n^2 , suggesting a second-order process. A term that compares the probability of recombination at level m to that at level g and the typical amount of time an electron spends in level m connected to the constant. More thought is required for the constant S . S is typically referred to as the pre-exponential component, but attempt-to-escape frequency is more appropriate (Hashim *et al.*, 2017). The number of times per second that an electron interacts with the lattice is multiplied by a transition probability, K , by a component that accounts for the change in entropy ΔS brought on by the transition from TO to e . This definition of s is based on simple models for electron localisation in a potential well. s can be written as a result.

$$s = \nu k e^{\left\{\frac{\Delta S}{k}\right\}} \quad (12)$$

Therefore, it is expected that s will have a value close to the lattice vibrational frequency or 10^{12} – 10^{14} s^{-1} . In the processes addressed in this review, the excited state e is frequently a delocalised band (i.e., the conduction band for electrons or the valence band for holes). Under these circumstances, the frequency factor can also be equivalent to the capture cross-

section of the metastable state based on careful balance reasoning, resulting in

$$s = N_s \nu \sigma \quad (13)$$

N stands for the functional density of states in the interlayer band, while ν stands for the thermal velocity of the free carrier. Because JV , ν , and σ are all temperature dependent, s is also temperature dependent (Bengisu, 2016).

Randall and Wilkins modified the previous general explanation of phosphorescence to fit the solids band theory (Vallejo *et al.*, 2020). The electronic transitions between delocalised bands and localised states, the latter caused by stoichiometric deviations within the host lattice due to impurities and other lattice faults, are used in this example to show how phosphorescence from insulators and semiconductors occurs (Kindrat *et al.*, 2014).

Applications of thermoluminescence

Archaeological Uses of Thermoluminescence: Ancient ceramic sample dating has been accomplished using thermoluminescence (Rüssel, 1999). The following justify the appropriateness of this strategy:

- i) The other techniques rely on the pottery shape and style to connect with the civilisation it belongs to while providing the precise date of the sample kiln firings.
- ii). Although TL dating can go back more than 30,000 years, the maximum age is only five years with just a year of precision.
- iii) Counterfeit can be easily, rapidly validated, and spotted using this technology.

The TL/OSL dating is carried out on a quartz grain extracted from brick or pottery by reading the TL-output. Most of the specimen TL is caused by TL-sensitive mineral additions, primarily quartz, in the host clay matrix of the pottery. The method used to date pottery is quite like that of geological materials. In archaeology, the kiln fire is a more precise and definite event. A long time ago, the kiln had to have been used to fire the pottery. This occurrence started the TL clock for archaeological dating (P. M. and D. V. Reddy, 2012). Any TL trapped inside the mineral inclusion during kiln burning due to internal and external irradiation throughout geological time (since crystallisation) is released.

Following the start of the TL clock (kiln fire), the pottery starts to accumulate TL because of internal radioactive emission from uranium (U), thorium (Th), and potassium (K) components in the clay as well as external radiations from the cosmic background at the excavation site. The average annual irradiation rate is 1 rad, with the majority originating from internal radiation and the remainder from soil and cosmic rays

(Hegde *et al.*, 2019). The specimen's overall irradiation rate can be calculated by dividing the accumulated TL by the total irradiation rate after the accumulation. TL has been measured and quantified regarding absorbed dosage using the appropriate calibration techniques. (Kawamura *et al.*, 2020). From there, the archaeological age can be calculated within equation (14);

$$\text{Age} = \frac{\text{Accumulated dose}}{\text{Annual dose rate}} \quad (14)$$

The age is determined by several intricate elements, though.

Ceramic artefacts must have acquired large doses of TSL during their geological or archaeological history to be estimated in age. Ceramics containing luminous minerals, mainly quartz and Feldspar, emit TSL proportional to their exposure time when heated after radiation exposure. The radiation is caused by cosmic rays and local gamma, beta, and alpha irradiation (due to traces of uranium, thorium, and potassium). Age = Natural TSL/ (TSL per unit dosage) x relates the age of the specimen to the "natural" signal (Natural dose rate). So, to evaluate age, one must first determine the organic TSL, then calibrate the TSL signal from the chemical to estimate the TSL per unit dosage, and lastly, choose the natural dose rate in the discovered site. The time since the TSL signal was last set to zero is the only factor that can be used to estimate age (Azorín *et al.*, 1993). Therefore, for the method to be effective, a "zeroing" event such as high-temperature heating (for example, when making pottery) or optical bleaching (for example, when sediment is deposited) must have occurred. Otherwise, the component mineral's geological age will be established by a TSL signal (Aydaş *et al.*, 2016).

Biology and biochemistry: The TL technique has gained popularity in studying biological and biochemical systems since all measurements must be done in the LNT-RT range. Hydroxy and aminobenzoic acids, proteins, nucleic acids, plant leaves, algae, and microbes have all been effectively studied (K *et al.*, 2017). It may be possible to correlate the TL behaviour of nucleic acids, proteins, and their constituent parts with the inter- and intramolecular transmission of radiation damage. The Z diagram's electron transport routes might be found to be connected to TL, and new routes could be defined (Wang *et al.*, 2017).

Forensic Science: The main objective of forensic science is the development and standardisation of methods for comparing evidence samples with components of a known source, which are typically

observable in minute quantities and must be inspected for strong intentions without causing damage. In several materials frequently used in criminal activity, such as glass, Earth, safe insulating traces, and so forth, thermoluminescence can be an intriguing strategy. When the TL traits do not match, it is possible to confidently conclude that a specific sample did not originate from a recognised source, known as exclusionary evidence (Bradley *et al.*, 2020; N. Itoh, 2002).

Examining the emission spectra, TL glow curves, and glow curves from materials that have undergone heavy synthetic gamma or X-ray exposure might help increase the reliability of TL observations by reducing the likelihood of coincidence matching (Duragkar *et al.*, 2019).

Geology: One of the first academic disciplines to apply the TL approach in various contexts was geology. These applications included mineralisation dating, igneous activity, sedimentation, and calculating the dunes' and beaches' expansion rates. When all other conventional procedures are unsuccessful, it has been demonstrated that the TL approach works well for dating geologically recent fossils (Ike *et al.*, 2021). The TL would begin to accumulate in a geological sample during crystallisation. It would typically earn until saturation because of the radionuclides contained in the minerals and other materials. The cumulative TL generally indicates the exposure rate to the environment at the location where the geological sample was taken if a low radioactive material (like quartz) is used. The UV component of natural light can impact the accumulation of TL. Geological events are dated using solar bleaching (Stokes, 2003). Since thermoluminescence is being bleached, it is only slightly reduced. These sun-bleached sand particles are shielded from further exposure to the sun once they have settled in a dune or beach. The radiation exposure to their new surroundings on a dune or beside the sea enables particles to get more TL (X.L. Wang, A.G. Wintle, 2007). Applying the single-grain method makes it possible to determine the age of geological materials 5% more or 5% less accurately.

Industry Quality Control: The first reference of TL's use to stabilise feldspars in ceramic products dates to 1938. When a ceramic is exposed to artificial radiation at trace levels, the amount of TL it emits is directly correlated with its feldspar content, and this is because any more quantitative study would take time (Itoh, 2002; K. and Reddy, 2008). As a result, any manageable variations in the feldspar levels may be verified quickly and effectively in the ceramic sector, where the same technique is carried out again to

manufacture similar things in batches. Specific surface catalysts, like Al_2O_3 , have TL sensitivities that make it quick and easy to assess their effectiveness. The TL released by these compounds may also be influenced by the lattice faults that allow adsorption processes, and the type and amount of TL may be positively correlated with catalytic activity (Duragkar *et al.*, 2019). The TL glow curve might then be employed as a standard for regulating the preparational conditions of a desired catalyst in such a situation. Theoretically, the TL method might be used to control the quality of many glass, ceramic, and semiconductor products; more recently, it was shown that minimal temperature TL glow curve adjustments in textile fibres could be related to structural variations and contaminants in the chemical tracer. However, industries have not paid attention to these (El-Faramawy *et al.*, 2021b).

Dosimetry of Radiation: Ionising radiations have been discovered to be highly beneficial to engineering, medicine, science, and technology in the modern scientific world. In every sphere of life, professionals use them (Alege *et al.*, 2022; Rabba *et al.*, 2023). In all applications, getting the desired effects depends critically on the precise amount of radiation energy absorption in the subjected material. Improved utilisation is essentially attainable by precisely measuring the radiation field absorbed energy and, if practical, the redistribution of this absorbed energy within the substance. Radiation dosimetry is built on measuring these parameters, and the devices used to do this are called dosimeters (Bengisu, 2016). Professionals have investigated and standardised various analytical techniques for calculating radiation doses (Efenji *et al.*, 2022). Some of the most effective methods that have been developed and employed include the following (O. B. Aljewaw *et al.*, 2023; El-Adawy *et al.*, 2010):

- Fluorescence-based method
- The diffuse reflectance method.
- Thermally induced luminescence method (TLD)
- Optical stimulation luminescence (OSL)
- EPR dosimetry is also known as electron paramagnetic resonance.

Thermoluminescence Dosimetry (TLD) is a technique that allows for the prediction of unknown radiation doses since the output of TL is exactly proportional to the intensity of the radiation dosage that the phosphor receives. Additionally, TL can provide a perfect passive measurement that considers integrated irradiation levels in years-long timescales. It results from massive implementation in the weekly, monthly, or yearly reported routine monitoring of radiation workers' exposures (Jaidass *et al.*, 2018). However,

some TL phosphors do not absorb energy like tissue when exposed to radiation, so it is difficult to reach the appropriate dosage that is important medically to a radiation worker in terms of protection. LiF , $\text{Li}_2\text{B}_4\text{O}_7$, BeO , and other almost tissue-equivalent phosphors carry out 4 points. better than more sensitive phosphors like CaSO_4 , CaF_2 , Mg_2SiO_4 , and others. For TLDs, numerous phosphors have been developed (Pal *et al.*, 2011). There are many uses for the TL-dosimeter. They are accommodating in various sectors because of their high sensitivity, compact size, range of exposure/dose coverage, reusability, and lack of sensitivity to external influences. The film badge strategy had already been used in actual practice by professionals. Later, they learned that the TLD strategy is better for several reasons. They thus created and implemented the TLD strategy throughout the previous three to four decades. In-vivo and phantom Dosimetry using dosimeters have been employed extensively in medical applications. Dosimeters for thermoluminescence can also be used to monitor radiation workers personally (P. M. and D. V. Reddy, 2012).

Due to their ability to integrate over extended times and evaluate shallow exposure, they are frequently used for environmental monitoring at a few micro-grey dosages. TLDs have been used in various applications for protection monitoring, including measurements of radiation leakage on and around source containers, measures of air scatter around open-top installations, area monitoring surrounding radiation installations, and others. The principal TL low-temperature peak of several phosphors, such as CaSO_4 : Dy, rapid fading ratio, has been used to calculate the duration of exposure after irradiation. (Duragkar *et al.*, 2019). It has also demonstrated that this method may measure thermal and fast neutron doses. It is possible to determine the gamma and thermal neutron exposure in a mixed field using a combination of dosimeters because thermal neutron-insensitive TL phosphors are also offered. TL dosimetry also includes non-ionising radiation dosimetry, including UV and microwave dosimetry, space dosimetry, and archaeology dating, which refers to ancient pottery and ceramics. A UV dosimeter can measure the thermal effectiveness of the UV energy if its sensitivity is like the thermal reactivity of human skin. TLDs, on the other hand, may be helpful in the agricultural sector. They are primarily employed in this sector for high-level photon dosimetry tasks like dose estimation for food preservation, seed sterilisation, insect management, etc. Traditionally, chemical dosimeters like the ferric (Fe^{2+} , Fe^{3+}) system were used to measure agriculture doses. TLDs are a less expensive method that can be

applied at dosage levels between 104 and 108 rad (Pekpak et al., 2014).

Individual Dosimetry: The primary goal of personnel dosimetry is to monitor the radiation dose supplied to personnel during ordinary work exposure. Examples are the nuclear industry, medical physicists and radiation technologists working in hospitals, industrial radiography, high-intensity gamma irradiators, and sailors on nuclear-powered warships (Furetta et al., 2001). According to recommendations from the International Atomic Energy Agency, it is envisaged that this monitoring will keep the exposure of such personnel below the permissible safety levels. ICRP is an acronym for the International Commission on Radiological Protection (Bengisu, 2016; Lewandowski, A. C. and McKeever, 1991). Being tissue-equivalent is one of the most crucial characteristics of any TLD in these applications. With a needed dosage estimate error of 10% to 20%, this field's intended dose equivalent range is 10⁻⁵ Sv to 10⁻¹ Sv (Stanković Petrović et al., 2021).

Dosimetry of the environment: Public anxiety around artificial radiation exposure, daylight gaseous radionuclide discharges from nuclear power plants, low-level waste disposal, nuclear fuel recycling, the likelihood of nuclear power station accidents, and nuclear power-related activities has increased in recent years (G.I. et al., 2014; Jamil, et al., 2023). Many nations have TLD systems close to atomic sites to control pre-operational levels (background levels) and levels just above background levels that may be related to the operation of these plants. The equivalency of tissues is not a problem. However, extensive exposure times are required due to the low exposure levels (typically 10⁻² mSv), making long-term stability and high sensitivity essential. The most crucial radiation sources are gamma emitters (Stanković Petrović et al., 2021).

Dosimetry in medicine: TLDs with correct covering and encapsulation have been placed in suitable apertures on the human body before the patient is exposed to ionising radiation during diagnostic and therapeutic procedures. This method has been utilised extensively in clinical research for a long time. Following that, the exposed TLDs are gathered and analysed. Doctors can use this information to suggest extra medicines based on the exact doses administered to crucial internal organs during these procedures. Other radiation dosimeters or detectors cannot provide this benefit (Rivera, 2012; Stanković Petrović et al., 2021). Diagnostic radiology, including X-ray exposure in mammography, dentistry, general health screening, and radiotherapy, are the uses of clinical radiation

exposure to humans (O. B. Aljewaw et al., 2023; Saidu et al., 2016). Radiation comes in various forms, such as X-rays with energies as low as 10 keV, gamma rays from ¹³⁷Cs or ⁶⁰Co, high-intensity photon beams with energies up to 25 MeV, electrons with energies up to 40 MeV, heavy charged particles, and neutrons. The range of radiation doses is 20 to 60 Gy, whereas dosages used in radiology are 10⁻⁵ to 10⁻² Gy. When estimating radiation therapy dosage, an accuracy of more than 3% is preferred because deviations that are more significant than this can harm treatment effects. Tissue equivalence is unquestionably the most essential requirement for employing a TLD material in this manner. High sensitivity is required to keep TLD dimensions as small as possible for in vivo evaluation. Because radiation doses can occasionally be relatively high, it is also preferable to have a linear dose-response over a more comprehensive dose range (Duragkar et al., 2019; Rivera, 2012).

Large Dose: Another illustration of the technology's numerous uses is the employment of TLDs exposed to high radiation dose detection, for instance, from 102 Gy to 106 Gy. Such massive doses could be encountered during material testing, food sterilisation, and nuclear reactor interiors (El-Adawy et al., 2010). However, the emergence of TLD sub-linearity may restrict the usage of traditional TLDs in these dosage ranges (saturation). This is because they seem to be saturated at more significant dose levels. Certain TLD materials with high-temperature peaks like CaSO₄: Dy and LiF: Mg, Ti- have been employed (Mhareb et al., 2016).

Dosimetry in retrospect: Creating novel and enhanced techniques for calculating the radioactivity dosage in places that have unintentionally been polluted is becoming increasingly popular worldwide. In this application, TSL methods have been applied for several years with varying degrees of success (Azorin et al., 1993). Examples include the Techa River in Russia and Chernobyl in Belarus and Ukraine, similar programs in Japan at Hiroshima and Nagasaki, and the United States at the Nevada bomb test site (Murthy, 2014).

The extra-terrestrial and terrestrial domains

Terrestrial Environment: With TL and OSL functioning as chronometers, geoscientists can ascertain the age of the most recent reset event. Everything might have been reset by heat, sunlight, or an abrupt spike in temperature during an earthquake. It is also possible to estimate the age of mineral formation by properly following sample protocols. This chronometer, made of Feldspar, gypsum, and other naturally occurring materials, can be used

everywhere. This technique has been used to understand historical volcanic eruptions, tsunamis, landslides, glacier movements, earthquakes, large floods, and other applications (K. and Reddy, 2008). The goal has been to utilise readily available materials on-site. TSL materials include pottery, porcelain, and other ceramic artefacts, which are helpful in this situation. These minerals can be used to recover quartz and Feldspar, and TSL dosimetry protocols are used to assess the absorbed dosage of these parts (K. and Reddy, 2008).

Dates from quartz: Compared to Feldspar, quartz is a more reliable material for luminescence dating. A few significant problems were found while dating with Feldspar, which may be the cause. Quartz has unique luminescence characteristics, making it possible to date it to 150 ka. Additionally, the TL peak at 325°C, as seen by the dosage response curve utilising OSL signals, is limited to that value since it frequently hits saturation at doses greater than 300 Gy. By stimulating the warmed sample with blue LEDs (to 240°C), OSL signal released in the 280-380 nm band is produced (47030 nm). The luminescence and trap centres of this signal are thought to be $[\text{TiO}_4/\text{Li}^+]_0$ and $[\text{AlO}_4]_0$, respectively (Itoh, 2002). There are several portions to this OSL decay signal, precisely seven (Monisha *et al.*, 2020). They are categorised as ultra-fast (UF), fast (F), medium (M), and slow components based on how quickly they bleach. Due to its speedy reactivation during movement and silt deposition by water or wind, the most popular and desired signal is quick. This signal was taken out to show how useful it is for dating tsunami sediments prone to incomplete bleaching (Amouzad *et al.*, 2016). However, this signal can only date sediments less than 150 ka old due to early saturation.

Analyses of dose distribution: Examining dose distribution to determine the paleo dose is an essential supplementary concern about the radiation dose acquired during burial. A few tens of aliquots were measured using the single aliquot SAR technique, and it is advised that the accurate paleo dose be chosen from this range (Balu *et al.*, 2016). The mean value of the paleo dose values will be overestimated if the grains were sparsely bleached during transit and deposition, causing the dose distribution to be right skewed (Murari, 2007). Single-grain dating was solved by choosing the grains from the sample that were most bleached. Yet another issue that the dating world had to deal with was beta-dose heterogeneity, in which not all single grains may respond to the beta dose similarly (Bengisu, 2016). The beta dosage range of the sediment matrix is around 1 mm, and the beta dose that grains with a diameter of 200 μm will get will

be heterogeneous, meaning that some grains will receive more doses than others. As a result, the dose distribution will be stretched further. Y.S. Mayya, P. proposed a "hotspot" model, and Morthekai, 2006, computed the spread as the number and position of feldspar grains in the matrix change (source of beta dosage). They discovered that the K concentration in the sediment influenced the spread (P. M. and D. V. Reddy, 2012). The distribution dispersion widens when the sediment contains 1.5% K. Feldspar grains began to have an impact in specific locations to overlap at K concentrations greater than 1.5%, necessitating further revision of their model by considering the ignored volume effects. M.K. Murari, H., and Achyuthan, 2007 extended this model using Monte Carlo simulations by including other situations, such as altering particle size, water content, and porosity in the sediment estimate using the SAR technique and a single aliquot. The core feature of SAR is that it employs test dose luminescence to correct the sensitivity shift brought on by pre-treatments, many readouts, and irradiations after each regenerative dosage (M.K. Murari, H. Achyuthan, 2007). However, because the test dosage is measured after the sensitivity has been modified, the first test dose modification cannot remedy the sensitivity change at the first luminescence readout (Kawamura *et al.*, 2020). The responsiveness is discovered using a method that requires correlating the low-temperature TL peaks before and after detecting natural luminescence. The technique is then utilised to account for the natural sensibility shift. NCF-SAR is the abbreviation for this improved SAR technology (natural sensitivity change corrected SAR). It has been shown that this provides precise ages from various samples. While not prevalent among all specimens, this natural diversity in sensitivity needs to be appropriately considered. It has been done at the single droplet level. Further research is required to determine how this effect appears at the single-grain level (Kron, 1995).

The thermo-chronology: (Lamothe, 2001) highlights the developments and constraints in feldspar luminescence, a low-temperature thermochronology-related emerging subject. One can utilise this method to investigate the thermal evolution of rocks or minerals. With a closure temperature of 55 to 80 degrees Celsius, (U-Th)/He is dated with apatite is currently the lowest temperature thermochronology method. OSL thermochronology, which employs quartz, has recently been proven to be a low temperature thermochronology advancement, with closure temperatures as low as 30-35 °C. To explain more recently and, as a result, shallow surface thermal history up to 2 kilometres, Feldspar can significantly

contribute by offering a method with additional low-temperature thermochronology (De Carvalho et al., 2012; M.K. Murari, H. Achyuthan, 2007). Currently, this is limited by the attempt-to-escape factors E and s values of feldspar luminescence signals, which are necessary for a certain trap depth, and the lack of a precise closure temperature. The existence of band tail states in Feldspar makes the studies erroneous, needing a new way of analysis for the TL, IRSL, ITL, and other curves, even if these values are already obtained through conventional analysis of the TL and IRSL curves. Furthermore, accurate prediction of the closure temperature requires first determining the nature of the aberrant dimming of luminescence signals, which is currently a work in progress (Swiontek et al., 2021).

Future of Feldspar: The scientific community faces difficulty because of the 0.4 eV extension below the conduction band of band-tail states. The standard analysis of TL, OSL, luminescence and other phenomena required reconsideration and modification because it predicted a pointed conduction band edge. The IRSL and anomalous fading have also recently been linked, with the former occurring via first higher energy states and subsequently band-tail states before recombination. The latter takes place by recombining ground states without IR stimulation. According to IR-stimulated electrons, there is a wide range of random hopping of the states of the tail band at the time before recombination. It has been tried to use a time-varying recombine probability to describe TL and IRSL. The difficulty lies in the potential inclusion of band-tail states (J. Chen, 2008; Salah, 2011).

Mineral and petroleum exploration: Mineral, oil, and natural gas exploration can use generated and naturally occurring thermal luminescence signals. In addition to good logging and geophysical studies to locate geological structures suitable for storing hydrocarbons, thermoluminescence investigations help establish the precise place to keep them. Even though many suggestions had been made, most had not yet been implemented (Rüssel, 1999). This could be because TL glow curves are complex and dependent on various outside factors, such as thermal leak, recrystallisation, and the addition or leaching of impurities into the target crystal. For this reason, thermoluminescence signals from minerals such as quartz, dolomite, and limestone can be used. Indicators include the glow curve peak's location, size, and form (Azorín et al., 1993).

Meteorites: Lamothe, 2001, emphasised how thermoluminescence has been utilised to characterise materials from planetary bodies, including meteorites,

samples that several missions have brought back from the Moon, and the anticipated minerals on Mars.

The temperature gradient of the Moon is calculated using thermoluminescence. It is also employed to estimate how long meteorite corpses have been on Earth after they split from their parent bodies and their cosmic exposure age. Feldspathic glass undergoes metamorphic devitrification, which increases Feldspar in typical chondrites (Lamothe, 2001). Therefore, the chondrite petrologic type can be determined using the sensitivity of these chondrites to Feldspar. Furthermore, it has been asserted that the change in peak temperature and rise in glow peak width contains details regarding the critical temperature to which it was previously heating up. It has been suggested that a paleothermometer caused this impact and is connected to an increase in Si-Al disorder in the crystal lattice. In general, thermoluminescence can be used to look into things like pre-atmospheric size, ablation rate, shock history, and orbital history (Ab Rasid et al., 2015). Careful sampling is necessary to leverage the intricately curved induced and natural TL light curves and extract meaningful information. Lately, a few writers have suggested using various optical emissions to establish exposure ages due to the reliance on paleo dose (De) and fading rate (g-value, %/decade) on cosmic exposure ages. Due to the fragile TL signal, future studies on small-sized meteorites and micrometeorites discovered the focus could also be on interplanetary dust particles gathered by stratospheric aircraft flights over Antarctica. It has been attempted to measure TL and OSL remotely from space bodies. (Ike et al., 2021).

Conclusion: This review provides a comprehensive overview of the structural properties of TLD materials and their preparation, application, and adaptability. The review highlights the importance of TLD materials in radiation dosimetry and their ability to measure low radiation doses accurately. The different types of TLD materials and their crystal structure have been discussed, along with their energy response and fading characteristics. The other methods used in preparing TLD materials have also been covered, along with their advantages and disadvantages. The review also highlights the various applications of TLDs in medical, environmental, and industrial radiation dosimetry. The adaptability of TLD materials to different dosimetry applications has been emphasised, and their potential use in the future has been discussed. Thermoluminescence, the salt crystals dosimetry properties from various sources, the application of thermoluminescence to cement exposed to a 10 Gy beta dose from a Sr-90 source, and the application of beta, X-ray, and gamma radiation to induce thermoluminescence in natural calcite material,

are all covered. TLD materials have shown to be a reliable and accurate method of calculating radiation doses, and they are still commonly employed in a range of industries where radiation exposure is a problem. A high range of TL response linearity, very low fading, and simple glow curves should all be goals in the hunt for new TL materials. Also, the TL mechanism is crucial and must be considered while creating new, practical materials for various purposes. TLD materials' structural characteristics are essential to their dosimetric performance, and several variables, including grain size, chemical composition, crystal structure, and annealing temperature, can change these characteristics. Finally, this review provides a valuable resource for researchers and practitioners in radiation dosimetry and highlights the potential of TLD materials in numerous applications.

Acknowledgments: The authors are grateful to Assoc. Prof. Dr. Iskandar Shahrim Bin Mustafa (Supervisor), the home institution, Federal University Lokoja (FUL), TETFund Nigeria, and all my research collaborators for the beautiful collection of articles. The authors extensively used existing papers by numerous authors in compiling the review paper and the grant account number 304.CSERC.6315568 funds for research efforts are also recognized.

REFERENCES

- Ab Rasid, A; Wagiran, H; Hashim, S; Ibrahim, Z; Ali, H (2015). Dosimetric properties of dysprosium doped lithium borate glass irradiated by 6MV photons. *Radiation Physics and Chemistry*, 112, 29–33. <https://doi.org/10.1016/j.radphyschem.2015.02.003>
- Alege, GO; Ojo, BH; Efenji, GI; Kachi, JB; Tawose, FO; Glen, E; Oladimeji, EO (2022). Cytogenetic Effects of Radiation from Projector on Meristematic Cells of Allium Cepa (Onions) Root. *Journal of Applied Sciences and Environmental Management*, 26(4), 737–744. <https://doi.org/10.4314/jasem.v26i4.25>
- Aljewaw, OB; Karim, MKA; Effendy, N; Kamari, HM; Zaid, MHM; Noor, NM; Salim, AA; Isa, NM; Kadir, ABA; Chew, MT; Abokridiga, AI (2023). Physical, optical and thermoluminescence properties of lithium aluminum borate glass co-doped with Dy₂O₃. *Radiation Physics and Chemistry*, 209(April), 111004. <https://doi.org/10.1016/j.radphyschem.2023.111004>
- Aljewaw, Osama Bagi; Karim, MKA; Kamari, HM; Zaid, MHM; Noor, NM; Isa, INC; Mhareb, MHA (2020). Impact of dy₂o₃ substitution on the physical, structural and optical properties of lithium–aluminium–borate glass system. *Applied Sciences (Switzerland)*, 10(22), 1–17. <https://doi.org/10.3390/app10228183>
- Aloraini, D. A; Sayyed, MI; Almuqrin, AAH; Kumar, A; Khazaalah, TH; Yasmin, S; Khandaker, MU; Baki, SO (2022). Preparation, radiation shielding and mechanical characterization of PbO–TeO₂–MgO–Na₂O–B₂O₃ glasses. *Radiation Physics and Chemistry*, 198(April), 110254. <https://doi.org/10.1016/j.radphyschem.2022.110254>
- Amouzad Mahdiraji, G; Dermosesian, E; Ghomeishi, M; Mahamd Adikan, FR (2016). Photonic Sensors: Glass Optical Fibers as Dosimeters. In *Reference Module in Materials Science and Materials Engineering* (Issue 1). Elsevier Ltd. <https://doi.org/10.1016/b978-0-12-803581-8.04077-7>
- Aydaş, C; Yüce, ÜR; Engin, B; Polymeris, GS; (2016). Dosimetric and kinetic characteristics of watch glass sample. *Radiation Measurements*, 85, 78–87. <https://doi.org/10.1016/j.radmeas.2015.12.030>
- Aydin, T; Demirtaş, H; Aydin, S (2013). TL/OSL studies of Li₂B₄O₇:Cu dosimetric phosphors. *Radiation Measurements*, 58, 24–32. <https://doi.org/10.1016/j.radmeas.2013.07.010>
- Azorín, J; Furetta, C; Scacco, A (1993). Preparation and properties of thermoluminescent materials. *Physica Status Solidi (A)*, 138(1), 9–46. <https://doi.org/10.1002/pssa.2211380102>
- Babu, AM; Jamalalah, BC; Kumar, JS; Sasikala, T; Moorthy, LR (2011). Spectroscopic and photoluminescence properties of Dy³⁺-doped lead tungsten tellurite glasses for laser materials. *Journal of Alloys and Compounds*, 509(2), 457–462. <https://doi.org/10.1016/j.jallcom.2010.09.058>
- Balu, L; Amaravel, R; Ezhil Pavai, R (2016). Effect of Zno on Physical, Structural and Mechanical Properties of B₂o₃ – Na₂o – Zno Glasses. *Journal of Applied Physics*, 8(6), 140–146. <https://doi.org/10.9790/4861-080603140146>
- Bengisu, M (2016). Borate glasses for scientific and industrial applications: a review. *Journal of Materials Science*, 51(5), 2199–2242. <https://doi.org/10.1007/s10853-015-9537-4>
- EFENJI, G. I; ISKANDAR, S. M; YUSOF, N. N; RABBA, J. A; MUSTAPHA, O. I; FADHIRUL, I. M; UMAR, S. A; KAMGBA, F. A; USHIE, P. O; MUNIRAH, J; THAIR, H. K; NABASU, S. E; HAYDER, S. N OKE, A O.

- Bootjomchai, C; Laopaiboon, R (2014). Thermoluminescence dosimetric properties and effective atomic numbers of window glass. *Nuclear Instruments and Methods in Physics Research, Section B: Beam Interactions with Materials and Atoms*, 323, 42–48. <https://doi.org/10.1016/j.nimb.2014.01.008>
- Bradley, DA; Khandaker, MU; Alanazi, A (2020). Irradiated glass and thermoluminescence yield: Dosimetric utility reviewed. *Radiation Physics and Chemistry*, 170(January), 108680. <https://doi.org/10.1016/j.radphyschem.2020.108680>
- De Carvalho, ÁB; Barros, TF; Guzzo, PL; Khoury, HJ (2012). Manufacturing polycrystalline pellets of natural quartz for applications in thermoluminescence dosimetry. *Materials Research*, 15(4), 536–543. <https://doi.org/10.1590/S1516-14392012005000075>
- Duragkar, A; Muley, A; Pawar, NR; Chopra, V; Dhoble, NS; Chimankar, OP; Dhoble, SJ (2019). Versatility of thermoluminescence materials and radiation dosimetry – A review. In *Luminescence* (Vol. 34, Issue 7, pp. 656–665). John Wiley and Sons Ltd. <https://doi.org/10.1002/bio.3644>
- Efenji, GI; Egeonu EK; Isah I; Onimisi SF; Uloko, FO; Nakale, JA; Ayua, KJ; Idris, MO (2022). Determination Of Activity Concentration Of Radioactive Elements In Borehole And Well Water Samples From Adankolo New Layout Lokoja. *FUDMA Journal of Sciences (FJS)*, 6(8.5.2017), 2003–2005. www.aging-us.com
- Efenji, GI; Mustafa, IS; Kamgba, FA; Ogunleye, OO; Khazaalah, TH; Ezra, NS; Naeem, HS; Shariff, HM; Jamil, M; Abdul Malik, MFI (2023). Description and dosimetric features of lithium borate glass doped with transition metals for thermoluminescence, a re-evaluation. *Physica Scripta*, 98(5). <https://doi.org/10.1088/1402-4896/acc23c>
- El-Adawy, A; Khaled, NE; El-Sersy, AR; Hussein, A; Donya, H (2010). TL dosimetric properties of Li₂O-B₂O₃ glasses for gamma dosimetry. *Applied Radiation and Isotopes*, 68(6), 1132–1136. <https://doi.org/10.1016/j.apradiso.2010.01.017>
- El-Egili, K; Oraby, AH (1996). The structure and electrical properties of lithium borate glasses containing thallic oxide. *Journal of Physics Condensed Matter*, 8(46), 8959–8970. <https://doi.org/10.1088/0953-8984/8/46/003>
- El-Faramawy, N; El-Naggar, A; Woda, C; El-Kinawy, M (2021a). Dosimetric properties of lithium borate glass doped with dysprosium. *Luminescence*, 36(1), 210–214. <https://doi.org/10.1002/bio.3937>
- El-Faramawy, N; El-Naggar, A; Woda, C; El-Kinawy, M (2021b). Investigation of TL dosimetric parameters of lithium borate glass doped with dysprosium. *Optical Materials*, 113(October 2020), 110672. <https://doi.org/10.1016/j.optmat.2020.110672>
- Furetta, C; Prokic, M; Salamon, R; Prokic, V; Kitis, G (2001). Dosimetric characteristics of tissue equivalent thermoluminescent solid TL detectors based on lithium borate. *Nuclear Instruments and Methods in Physics Research, Section A: Accelerators, Spectrometers, Detectors and Associated Equipment*, 456(3), 411–417. [https://doi.org/10.1016/S0168-9002\(00\)00585-4](https://doi.org/10.1016/S0168-9002(00)00585-4)
- Efenji, GI; Obi, EO; Kamgba, FA; Odesanya, I (2014). Gas flaring effects on temperature change in Amai Community area in Niger Delta region of Nigeria. *IOSR Journal of Applied Physics*, 6(2), 40–45. <https://doi.org/10.9790/4861-06234045>
- Godwin, E; Iskandar, SM; Ferdinand, K; Ogunleye, K; Khazaalah, T; Salah Naeem, H; Ezra, NS; Abdul Malik, MFI; Jamil, M; Shariff, HM (2023). Description and dosimetric features of lithium borate glass doped with transition metals for thermoluminescence, a re-evaluation. *Physica Scripta*. <http://iopscience.iop.org/article/10.1088/1402-4896/acc23c>
- Hamzah, SA; Saeed, MA; Wagiran, H; Hashim, IH (2017). Thermoluminescence (TL) dosimeter of dysprosium doped strontium borate glass for different glass modifiers (Na, Li, Ca) subjected from 1 to 9 Gy doses. *EPJ Web of Conferences*, 156, 1–6. <https://doi.org/10.1051/epjconf/201715600007>
- Hashim, S; Alajerami, YSM; Ramli, AT; Ghoshal, SK; Saleh, MA; Abdul Kadir, AB; Saripan, MI; Alzimami, K; Bradley, DA; Mhareb, MHA (2014). Thermoluminescence dosimetry properties and kinetic parameters of lithium potassium borate glass co-doped with titanium and magnesium oxides. *Applied Radiation and Isotopes*, 91, 126–130. <https://doi.org/10.1016/j.apradiso.2014.05.023>
- EFENJI, G. I; ISKANDAR, S. M; YUSOF, N. N; RABBA, J. A; MUSTAPHA, O. I; FADHIRUL, I. M; UMAR, S. A; KAMGBA, F. A; USHIE, P. O; MUNIRAH, J; THAIR, H. K; NABASU, S. E; HAYDER, S. N OKE, A O.

- Hashim, S; Mhareb, MHA; Ghoshal, SK; Alajerami, YSM; Saripan, MI; Bradley, DA (2017). Luminescence features of dysprosium and phosphorus oxide co-doped lithium magnesium borate glass. *Radiation Physics and Chemistry*, 137(October 2016), 45–48. <https://doi.org/10.1016/j.radphyschem.2016.10.004>
- Hegde, V; Chauhan, N; Viswanath, CSD; Kumar, V; Mahato, KK; Kamath, SD (2019). Photoemission and thermoluminescence characteristics of Dy³⁺ - doped zinc sodium bismuth borate glasses. *Solid State Sciences*, 89(November 2018), 130–138. <https://doi.org/10.1016/j.solidstatesciences.2019.01.002>
- Himamaheswara Rao; Syam Prasad, V; Mohan Babu, P; Venkateswara Rao, M; Satyanarayana, P; Luís F, T; Veeraiah, SN (2018). Spectroscopic studies of Dy³⁺ ion doped tellurite glasses for solid state lasers and white LEDs. *Spectrochimica Acta - Part A: Molecular and Biomolecular Spectroscopy*, 188, 516–524. <https://doi.org/10.1016/j.saa.2017.07.013>
- Ichoja, A; Hashim, S; Ghoshal, SK; Hashim, IH; Omar, RS (2018). Physical, structural and optical studies on magnesium borate glasses doped with dysprosium ion. *Journal of Rare Earths*, 36(12), 1264–1271. <https://doi.org/10.1016/j.jre.2018.05.013>
- Ike, PO; Folley, DE; Agwu, KK; Chithambo, ML; Chikwembani, S; Ezema, FI (2021). Influence of dysprosium doping on the structural, thermoluminescence and optical properties of lithium aluminium borate. *Journal of Luminescence*, 233(August 2020), 117932. <https://doi.org/10.1016/j.jlumin.2021.117932>
- J. Chen; XL; ZY (2008). Baota landslide in the Three Gorges area and its OSL dating. *Environmental Geology*, 54, 417–425.
- Jaidass, N; Krishna Moorthi, C; Mohan Babu, A; Reddi Babu, M (2018). Luminescence properties of Dy³⁺ doped lithium zinc borosilicate glasses for photonic applications. *Heliyon*, 4(3), e00555. <https://doi.org/10.1016/j.heliyon.2018.e00555>
- Jamil, M; Mustafa, IS; Ahmed, NM; Sahul Hamid, SB; Khazaalah, TH; Godwin, E; Ezra, NS; Salah, HN; (2023). Poly(ethylene) oxide/erbium oxide as T2 and T1-T2 dual-mode MRI diagnostic nanofibres. *Ceramics International*, 49(13), 22429–22439. <https://doi.org/https://doi.org/10.1016/j.ceramint.2023.04.072>
- Jamil, M; Mustafa, IS; Sahul Hamid, SB; Ahmed, NM; Khazaalah, TH; Godwin, E; Ezra, NS; Salah, HN (2023). Parameterisation and cellular evaluation of poly(ethylene) oxide-coated erbium oxide in MCF-7 cells as MRI diagnostic nanofibres. *Colloids and Surfaces B: Biointerfaces*, 228(June), 113423. <https://doi.org/10.1016/j.colsurfb.2023.113423>
- K, EE; Osahon, OD; Efenji, GI (2017). *Comparative Assessment of Electrical Properties and pH of Homemade and Industrial Pineapple Juice Samples from Benin City*. 3(2), 1–9.
- Kaur, A; Khanna, A; Aleksandrov, LI (2017). Structural, thermal, optical and photo-luminescent properties of barium tellurite glasses doped with rare-earth ions. *Journal of Non-Crystalline Solids*, 476(August), 67–74. <https://doi.org/10.1016/j.jnoncrysol.2017.09.025>
- Kawamura, I; Kawamoto, H; Fujimoto, Y; Koshimizu, M; Okada, G; Koba, Y; Ogawara, R; Suda, M; Yanagida, T; Asai, K (2020). Thermoluminescence properties of Dy³⁺-doped CaO–Al₂O₃–B₂O₃ glasses for neutron detection. *Nuclear Instruments and Methods in Physics Research, Section B: Beam Interactions with Materials and Atoms*, 468(January), 18–22. <https://doi.org/10.1016/j.nimb.2020.02.015>
- Khazaalah, TH; Mustafa, IS; Sayyed, MI (2022). Radiation parameterizations and optical characterizations for glass shielding composed of SLS waste glass and lead-free materials. *Nuclear Engineering and Technology*, xxxx. <https://doi.org/10.1016/j.net.2022.08.009>
- Kindrat, II; Padlyak, BV; Protsiuk, VO; Drzewiecki, A; Adamiv, VT; Burak, YV; Teslyuk, IM (2014). Optical spectroscopy of borate glasses, doped with europium. *International Conference on Oxide Materials for Electronic Engineering - Fabrication, Properties and Applications, OMEE 2014 - Book of Conference Proceedings*, 141–142. <https://doi.org/10.1109/OMEE.2014.6912379>
- Kron, T; (1995). Thermoluminescence dosimetry and its applications in medicine--Part 2: History and applications. *Australasian Physical & Engineering Sciences in Medicine / Supported by the Australasian College of Physical Scientists in Medicine and the Australasian Association of*
- Efenji, G. I; Iskandar, S. M; Yusof, N. N; Rabba, J. A; Mustapha, O. I; Fadhurul, I. M; Umar, S. A; Kamgba, F. A; Ushie, P. O; Munirah, J; Thair, H. K; Nabasus, S. E; Hayder, S. N Oke, A. O.

- Physical Sciences in Medicine*, 18(1), 1–25.
<https://doi.org/10.1007/13246.1879-5447>
- Owen, LA; Kampb, U; Spencer, JQ; KH (2002). A review and revision of the glacial chronology based on new optically stimulated luminescence dating. *Quaternary International*, 97–98, 41–55.
- Lamothe, DJH; M (2001). Ubiquity of anomalous fading in K-feldspars and the measurement and correction for it in optical dating. *Canadian Journal of Earth Sciences*, 38, 1093–1106.
- Lewandowski, AC; McKeever, SWS (1991). Generalized description of thermally stimulated processes without quasiequilibrium approximation. *Phys. Rev., B*, 43, 8163–8178.
- Lim, TY; Wagiran, H; Hussin, R; Hashim, S (2015). Thermoluminescence response of dysprosium doped strontium tetraborate glasses subjected to electron irradiations. *Applied Radiation and Isotopes*, 102, 10–14.
<https://doi.org/10.1016/j.apradiso.2015.04.005>
- Murari, MK; Achyuthan, H; AKS (2007). Luminescence studies on the sediments laid down by the December 2004 tsunami event: Prospects for the dating of palaeo-tsunamis and for the estimation of sediment fluxes. *Curr. Sci.*, 92, 367–371.
- McKeever, RC; SWS (1997). Theory of Thermoluminescence and Related Phenomena. *World Scientific, Singapore*.
- Mhareb, MHA; Hashim, S; Ghoshal, SK; Alajerami, YSM; Bqoor, MJ; Hamdan, AI; Saleh, MA; Karim, MKB, A (2016). Effect of Dy₂O₃ impurities on the physical, optical and thermoluminescence properties of lithium borate glass. *Journal of Luminescence*, 177, 366–372.
<https://doi.org/10.1016/j.jlumin.2016.05.002>
- Mishra, L; Sharma, A; Vishwakarma, AK; Jha, K; Jayasimhadri, M; Ratnam, BV; Jang, K; Rao, AS; Sinha, RK (2016). White light emission and color tunability of dysprosium doped barium silicate glasses. *Journal of Luminescence*, 169, 121–127.
<https://doi.org/10.1016/j.jlumin.2015.08.063>
- Monisha, M; D'Souza, A, N; Hegde, V; Prabhu, NS; Sayyed, MI; Lakshminarayana, G; Kamath, SD (2020). Dy³⁺ doped SiO₂–B₂O₃–Al₂O₃–NaF–ZnF₂ glasses: An exploration of optical and gamma radiation shielding features. *Current Applied Physics*, 20(11), 1207–1216.
<https://doi.org/10.1016/j.cap.2020.08.004>
- Murthy, KVR (2014). Thermoluminescence and its applications: A review. *Defect and Diffusion Forum*, 347, 35–73.
<https://doi.org/10.4028/www.scientific.net/DDF.347.35>
- N, Itoh; DS; AMS (2002). Ionic and electronic processes in quartz: Mechanisms of thermoluminescence and optically stimulated luminescence. *J. of Appl. Phys*, 92, 5036–5045.
- Pal, M; Roy, B; Pal, M (2011). Structural Characterization of Borate Glasses Containing Zinc and Manganese Oxides. *Journal of Modern Physics*, 02(09), 1062–1066.
<https://doi.org/10.4236/jmp.2011.29129>
- Pawar, PP; Munishwar, SR; Gautam, S; Gedam, RS (2017). Physical, thermal, structural and optical properties of Dy³⁺ doped lithium alumino-borate glasses for bright W-LED. *Journal of Luminescence*, 183, 79–88.
<https://doi.org/10.1016/j.jlumin.2016.11.027>
- Pekpak, E; Yilmaz, A; Ozbayoglu, G (2014). An Overview on Preparation and TL Characterization of Lithium Borates for Dosimetric Use. *The Open Mineral Processing Journal*, 3(1), 14–24.
<https://doi.org/10.2174/1874841401003010014>
- Prabhu, NS; Sharmila, K.; Kumaraswamy, S; Somashekarappa, HM; Sayyed, MI; Al-Ghamdi, H; Almuqrin, AH; Kamath, SD (2021). An examination of the radiation-induced defects and thermoluminescence characteristics of Sm₂O₃ doped BaO–ZnO–LiF–B₂O₃ glass system for γ -dosimetry application. *Optical Materials*, 118(April), 111252.
<https://doi.org/10.1016/j.optmat.2021.111252>
- Rabba, JA; Uloko, FO; Efenji, GI; Eghaghe, SO; Jaafar, HA; Jafri, MZM; Osman, ND (2023). Assessment of Correlation between Dimensions of Ball Phantom and Distortion Rate of Panoramic Radiography in Dental Cone Beam Computed Tomography. *Journal of Applied Sciences and Environmental Management*, 27(11), 2469–2474.
<https://doi.org/10.4314/jasem.v27i11.15>
- Rao, GV; Reddy, PY; Veeraiah, N (2002). Thermoluminescence studies on Li₂O–CaF₂–B₂O₃ glasses doped with manganese ions. *Materials Letters*, 57(2), 403–408.
- EFENJI, G. I; ISKANDAR, S. M; YUSOF, N. N; RABBA, J. A; MUSTAPHA, O. I; FADHIRUL, I. M; UMAR, S. A; KAMGBA, F. A; USHIE, P. O; MUNIRAH, J; THAIR, H. K; NABASU, S. E; HAYDER, S. N OKE, A O.

- [https://doi.org/10.1016/S0167-577X\(02\)00800-5](https://doi.org/10.1016/S0167-577X(02)00800-5)
- Ravikumar, N; Arun Kumar, R; Panigrahi, BS; Madhusoodanan, U; Palan, CB; Omanwar, SK (2018). Spectral and thermoluminescence characteristics of high gamma dose irradiated Dy:LiKB4O7 single crystals. *Nuclear Instruments and Methods in Physics Research, Section B: Beam Interactions with Materials and Atoms*, 436(September), 203–210. <https://doi.org/10.1016/j.nimb.2018.09.040>
- Razak, NA; Hashim, S; Mhareb, MHA; Tamchek, N (2016). Photoluminescence and thermoluminescence properties of Li₂O-Na₂O-B₂O₃ glass. In *Luminescence* (Vol. 31, Issue 3, pp. 754–759). <https://doi.org/10.1002/bio.3020>
- Reddy, KVRM; J, N (2008). Thermoluminescence: Basic Theory Application and Experiment. *Publ. Nucleonix, Hyderabad*.
- Reddy, PM; DV (2012). Applications of TL and OSL in terrestrial and extra-terrestrial materials: recent developments and challenges. *International Journal of Luminescence and Applications*, 2(3), 96-108.
- Rivera, T (2012). Thermoluminescence in medical dosimetry. *Applied Radiation and Isotopes*, 71(SUPPL.), 30–34. <https://doi.org/10.1016/j.apradiso.2012.04.018>
- Rüssel, C (1999). Introduction to Glass Science and Technology. In *Zeitschrift für Physikalische Chemie* (Vol. 208, Issues 1–2). https://doi.org/10.1524/zpch.1999.208.part_1_2.2_92
- Saidu, A; Wagiran, H; Saeed, MA; Alajerami, YSM (2015). Thermoluminescence characteristics of zinc lithium borate glass activated with Cu⁺ (ZnO–Li₂O–B₂O₃:Cu⁺) for radiation dosimetry. *Journal of Radioanalytical and Nuclear Chemistry*, 304(2), 627–632. <https://doi.org/10.1007/s10967-014-3846-y>
- Saidu, A; Wagiran, H; Saeed, MA; Alajerami, YSM; Kadir, ABA; (2016). Effect of co-doping of sodium on the thermoluminescence dosimetry properties of copper-doped zinc lithium borate glass system. *Applied Radiation and Isotopes*, 118(September), 375–381. <https://doi.org/10.1016/j.apradiso.2016.10.005>
- Saidu, A; Wagiran, H; Saeed, MA; Obayes, HK; Bala, A; Usman, F (2018). Thermoluminescence response of rare earth activated zinc lithium borate glass. *Radiation Physics and Chemistry*, 144(August 2017), 413–418. <https://doi.org/10.1016/j.radphyschem.2017.10.004>
- Salah, N (2011). Nanocrystalline materials for the dosimetry of heavy charged particles: A review. *Radiation Physics and Chemistry*, 80(1), 1–10. <https://doi.org/10.1016/j.radphyschem.2010.08.003>
- Salama, E; Soliman, HA (2018). Thermoluminescence glow curve deconvolution and trapping parameters determination of dysprosium doped magnesium borate glass. *Radiation Physics and Chemistry*, 148(March), 95–99. <https://doi.org/10.1016/j.radphyschem.2018.03.003>
- Sani, SFA; Othman, MHU; Alqahtani, A; Almgren, KS; Alkallas, FH; Bradley, DA (2020). Low-cost commercial borosilicate glass slides for passive radiation dosimetry. *PLoS ONE*, 15(12 December), 1–16. <https://doi.org/10.1371/journal.pone.0241550>
- Sanyal, B; Goswami, M; S, S; Prakasan, V; Krishnan, M; Ghosh, SK (2019). Thermoluminescence and electron paramagnetic resonance study on rare earth/transition metal doped lithium borate glasses for dosimetry applications. *Journal of Luminescence*, 216(August), 116725. <https://doi.org/10.1016/j.jlumin.2019.116725>
- Sanyal, B; Goswami, M; Shobha, S; Prakasan, V; Chawla, SP; Krishnan, M; Ghosh, SK (2017). Synthesis and characterization of Dy³⁺ + doped lithium borate glass for thermoluminescence dosimetry. *Journal of Non-Crystalline Solids*, 475(August), 184–189. <https://doi.org/10.1016/j.jnoncrysol.2017.09.016>
- Singh, R; Kainth, HS (2018). Effect of heating rate on thermoluminescence output of LiF: Mg, Ti (TLD-100) in dosimetric applications. *Nuclear Instruments and Methods in Physics Research, Section B: Beam Interactions with Materials and Atoms*, 426(April), 22–29. <https://doi.org/10.1016/j.nimb.2018.04.025>
- Stanković Petrović, JS; Knežević, ŽI; Kržanović, NL; Majer, MC; Živanović, MZ; Ciraj-Bjelac, OF (2021). Review of the thermoluminescent dosimetry method for the environmental dose
- EFENJI, G. I; ISKANDAR, S. M; YUSOF, N. N; RABBA, J. A; MUSTAPHA, O. I; FADHIRUL, I. M; UMAR, S. A; KAMGBA, F. A; USHIE, P. O; MUNIRAH, J; THAIR, H. K; NABASU, S. E; HAYDER, S. N OKE, A O.

- monitoring. *Nuclear Technology and Radiation Protection*, 36(2), 150–162. <https://doi.org/10.2298/NTRP2102150S>
- Stokes, MF; S (2003). Dating volcanic and related sediments by luminescence methods: A review. *Earth Sci. Rev*, 64, 229–264
- Sundararaman, S; Huang, L; Ispas, S; Kob, W (2020). New interaction potentials for borate glasses with mixed network formers. *J. Chem. Phys.* 152(10). <https://doi.org/10.1063/1.5142605>
- Świontek, S; Środa, M; Gieszczyk, W (2021). Ceramics, glass and glass-ceramics for personal radiation detectors. *Materials*. 14(20). <https://doi.org/10.3390/ma14205987>
- Thomas, S; Chithambo, ML (2017). Kinetic analysis and general features of thermoluminescence of B₂O₃-Li₂O-ZnF₂ glass. *Radiation Measurements*, 100, 1–8. <https://doi.org/10.1016/j.radmeas.2017.03.038>
- Ntwaeaborwa, OM (2019). The influence of dopants on thermoluminescence of Sr₂MgSi₂O₇. *J. Luminescence*. 208(December 2018), 104–107. <https://doi.org/10.1016/j.jlumin.2018.12.035>
- Vallejo, MA; Elias, JA; Honorato, M; Ceron, PV; Gomez-Solis, C; Wiechers, C; Navarro, R, Sosa, M (2020). Silver Nanoparticles Enhance Thermoluminescence and Photoluminescence Response in Li₂B₄O₇ Glass Doped with Dy³⁺ and Yb³⁺. *J. Fluorescence*, 30(1), 143–150. <https://doi.org/10.1007/s10895-019-02479-w>
- Wang, S; Du, X; Jing, Y; Guo, Y; Deng, T (2017). Solid-liquid phase equilibrium in the ternary systems (Li₂B₄O₇ + MgB₄O₇ + H₂O) and (Na₂B₄O₇ + MgB₄O₇ + H₂O) at 298.15 K. *J. Chem. Engineer. Data*. 62(1), 253–258. <https://doi.org/10.1021/acs.jced.6b00626>
- Wang, XL; Wintle, AG; YCL (2007). Testing a single-aliquot protocol for recuperated OSL dating. *Radiat. Meas*, 42, 380–391

Thomas, S; Kalita, JM; Chithambo, ML;

EFENJI, G. I; ISKANDAR, S. M; YUSOF, N. N; RABBA, J. A; MUSTAPHA, O. I; FADHIRUL, I. M; UMAR, S. A; KAMGBA, F. A; USHIE, P. O; MUNIRAH, J; THAIR, H. K; NABASU, S. E; HAYDER, S. N OKE, A O.